Current Hysteresis Control of High Step-up Current-fed DC-DC Converter for Haptic Application

Zhen Wu[1,2], Shizhen Huang[1,2], Nan Li[1,2] and Tao Zeng[1, 2*]

[1]Dept. Instrumental and Electrical Engineering, Xiamen University, Xiamen, China
[2]Shenzhen Research Institute of Xiamen University, Shenzhen, China
[*]Corresponding author

Abstract—The steady accuracy of output waveforms is a core index for judging the performance of DC-DC converter and it is mainly determined by the control scheme of DC-DC converter. This paper studied a PWM current hysteresis control scheme to improve the performance of the high step-up current-fed DC-DC converter proposed in our previous work. This control scheme treated the currents of two input inductors as control quantities, and treated the error between the practical and theoretical output voltage as feedback quantity. It calculated the reference current of input inductor by collecting the output voltage and current of the DC-DC converter, and adjusted the hysteresis band width in real time. A control system including the DC-DC converter and the current hysteresis control circuit has been presented and evaluated. The simulation results demonstrates its easy-implementation, fast response, and high steady accuracy of 97%.

Keywords- current-fed DC-DC converter; current hysteresis control; steady accuracy

I. INTRODUCTION

As the development of power electronics, various DC-DC converters with high performance have been proposed and applied [1, 2]. The steady accuracy of the output voltage waveform is one of the most important output performances of the DC-DC converter, and it is largely determined by the control scheme.

Research activities have proposed different control schemes according to different DC-DC converters, such as adaptive control, sliding mode control, fuzzy control, and hysteresis control, etc. The adaptive control schemes update model parameters and adjust the duty cycle in real time according to the parameter updating rules, which greatly improves the control accuracy and ensures high robustness to external disturbance. However, it is hard to achieve general application because the adaptive module is really difficult to realization [3, 4]. Sliding mode control achieves discontinuous switching from one system structure to the other. It is known for its strong robustness and quick dynamic response to system parameters and load disturbance. Nevertheless, it is hard to switch to accurate switching surface due to the inertia of sliding module and the time lag of transmission system, which causes drastic system chattering and high output voltage ripple [5-7]. The fuzzy control schemes realize their function by changing the language rules of the controller rather than modeling an accurate mathematical controller, refraining from cumbersome modeling process of complex control system. This method is provided with simple algorithm, short running time and good robustness. However, the development of the language rules completely depends on a large number of experiments and extensive experience of designers. Some problems like low accuracy and low adaptive ability greatly prevent the application of the fuzzy control [8, 9]. In contrast, PWM hysteresis control is a highly practical method which generates PWM driving signals of switches by comparing control quantity (output voltage or current of inductor) with given threshold (or hysteresis band width). The state of switch will change when the control quantity is larger than the upper threshold or smaller than the lower threshold, and it will keep on when the control quantity is between the lower threshold and the upper threshold. The PWM hysteresis control is widely used for its fast response, high stability and high accuracy of output waveforms.

This paper proposed a PWM current hysteresis control scheme applied on a high step-up DC-DC converter presented in our previous work [10], by considering the ripple characteristic of the input inductor current, the input voltage and the output voltage. Unlike the hysteresis control scheme shown in [11-13], this PWM current hysteresis control scheme treated the current of two input inductors as control quantities, and the error between the practical and theoretical output voltage as feedback quantity. The reference current of input inductor can be calculated by collecting the output voltage and current of the DC-DC converter, and the hysteresis band width will be adjusted in real time. The simulation results have verified that the proposed PWM current hysteresis control method could obtain fast response and high steady accuracy up to 97%.

The paper is organized in the following manner. Section II develops the high step-up current-fed DC-DC converter and the proposed current hysteresis control scheme. Section III presents the simulation results, and section IV summarizes the conclusions.

II. DC-DC CONVERTER AND THE PROPOSED CURRENT HYSTERESIS CONTROL SCHEME

A. The Proposed Current Hysteresis Control System

The current hysteresis control system of the high step-up current-fed DC-DC converter is composed of a DC-DC

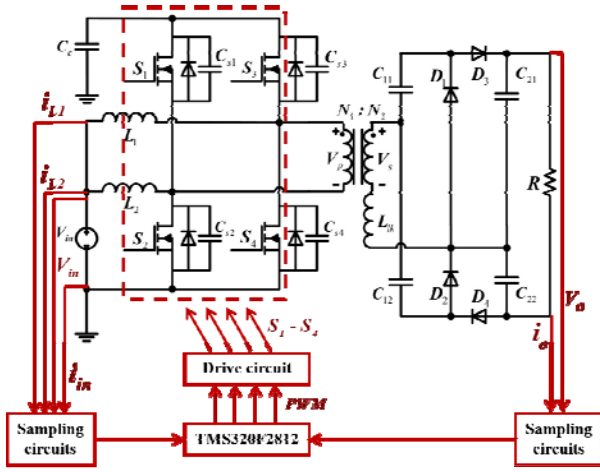converter circuit and its current hysteresis control circuit, as shown in Figure 1.

FIGURE I. HIGH STEP-UP CURRENT-FED DC-DC CONVERTER WITH THE PROPOSED HYSTERESIS CONTROL

The high step-up current-fed DC-DC converter consists of two input inductors L_1 and L_2, a clamp capacitor C_c, two switch bridges (S_1 and S_2 compose the first bridge while S_3 and S_4 compose the second bridge), four rectifier diodes D_1 to D_4, a resonant inductor L_{lk}, two resonant capacitors C_{11} and C_{12}, two output capacitors C_{21} and C_{22}, a load R, and an isolating transformer with ratio $N=1$. The pulse-width modulation plus phase angle shift (PPAS) is employed as the drive scheme for four switches, and it is noted that one power switch S_1 (or S_3) of each bridge is driven complementarily by the other S_2 (or S_4), and the phase difference between two bridges keeps at a constant 180°. Our previous work has proved that this DC-DC converter has the benefits of high gain, low ripple of input current and output voltage, low switching loss, and high conversion efficiency.

The input voltage, the input current, the output voltage and the output current are sampled by sensors of the current hysteresis control circuit. The reference current and the hysteresis band width are calculated and four PWM signals are exported by micro controller. The driving signals of four switches then will be obtained by the isolated drive circuit. Unlike the conventional hysteresis control method, the current hysteresis control circuit in this paper works with a DSP-TMS320F2812, which promises a higher flexibility, stronger anti-interference ability and higher stability of the DC-DC converter.

B. Operation Stage Analysis

The steady-state operation of the DC-DC converter can be divided into 3 stages during a switching period according to the state change of switches S_2 and S_4, as shown in Figure 2.

Stage1: as shown in Figure 2(A), it forms two conduction loops V_{in}, L_2, S_2 and V_{in}, L_1, S_4 when the switches S_2 and S_4 are in the on-state. The voltage of inductor L_2 and L_1 keeps on V_{in}, and the current i_{L1} and i_{L2} increases linearly.

Stage2: as shown in Figure 2(B), it forms two conduction loops V_{in}, L_2, S_1, C_C and V_{in}, L_2, T, S_4 when S_2 is in the off-state and S_4 is in the on-state. The voltage of inductor L_2 keeps on $V_{in}-V_{Cc}$, where V_{Cc} is the clamping voltage of capacitor C_c. The current i_{L2} decreases linearly. In addition, there are two resonant loops on the secondary winding of the transformer, L_{lk}, C_{11}, D_1 and $L_{lk}, C_{12}, D_4, C_{22}$, respectively.

Stage3: as shown in Figure 2(C), it forms two conduction loops V_{in}, L_1, S_3, C_C and V_{in}, L_1, T, S_2 when S_2 is in the on-state and S_4 is in the off-state. The voltage of inductor L_1 keeps on $V_{in}-V_{Cc}$. The current i_{L1} decreases linearly. Similarly, there are two resonant loops on the secondary winding of the transformer, L_{lk}, C_{12}, D_2 and $L_{lk}, C_{11}, D_3, C_{21}$, respectively.

The waveforms of the DC-DC converter during a switching period are shown in Figure 3. Taking the second bridge for example, the inductor current i_{L1} increases linearly when S_4 is in the on-state (T_{on1} in Figure 3) while decreases linearly when S_4 is in the off-state (T_{off1} in Figure 3). It is obvious that the change of inductor current i_{L1} and the switching states of S_4 are synchronous, so that the driving signals of the second bridge can be achieved by the current hysteresis control of the inductor current i_{L1}. Similarly, the change of inductor current i_{L2} and the switching states of S_2 are synchronous, and the driving signals of the first bridge can be achieved by the current hysteresis control of the inductor current i_{L2}.

The volt-second balance law of L_1 during one switching period determines the relationship between V_{in} and V_{Cc} as follows:

$$V_{in} \cdot D + (V_{in}-V_{Cc}) \cdot (1-D) = 0. \tag{1}$$

Thus, it can be deduced as:

$$V_{Cc}/V_{in} = \frac{1}{1-D}, \tag{2}$$

where, D is the duty of the switches S_2 and S_4. The volt-second balance law of L_{lk} during one switching period determines the relationship between the resonant capacitor average voltage V_{C11} and V_o as follow:

$$(V_{C11} + N \cdot V_{Cc} - \frac{V_o}{2}) \cdot \frac{T_0}{2} + (V_{C11} - N \cdot V_{Cc}) \cdot \frac{T_0}{2} = 0, \tag{3}$$

where, T_0 is the resonant period. The average voltages of the resonant capacitors V_{C11} and V_{C12} are obtained as the (4) in view of the symmetrical circuit:

$$V_{C11} = V_{C12} = 0.25V_o. \tag{4}$$

Since the average voltage V_{C11} is equal to the amplitude of v_s, and the amplitude of v_p is equal to V_{Cc}, it can be deduced that the relationship between V_{Cc} and V_o should be:

$$V_{Cc} = \frac{1}{4N} \cdot V_o .$$ (5)

By combining (2) and (5), it can be deduced that the relationship between input and output voltages is:

$$V_o / V_{in} = N \cdot \frac{4}{1-D} .$$ (6)

C. The Proposed Current Hysteresis Control Scheme

The proposed current hysteresis control scheme is presented in this section. The steady state analysis of the DC-DC converter is carried on to obtain the theoretical current of input inductor I_{ref} during a stable period. Based on the operation stages analysis in section B, the input inductor current during a period should be:

$$L\frac{di_{L1}}{dt} = V_{in} , \text{ when } S_4 \text{ on,}$$ (7)

$$L\frac{di_{L1}}{dt} = V_{in} - V_{Cc} , \text{ when } S_4 \text{ off.}$$ (8)

According to (7) and (8), the turn-on time T_{on1} and turn-off time T_{off1} can be calculated as (9) and (10), respectively.

$$T_{on1} = \frac{\Delta I_{L1} \cdot L_1}{V_{in}} ,$$ (9)

$$T_{off1} = \frac{\Delta I_{L1} \cdot L_1}{V_{Cc} - V_{in}} ,$$ (10)

where, ΔI_{L1} is the range of the input inductor current during a period. Thus, the period should be:

$$T_S = T_{on1} + T_{off1} = \Delta I_{L1} \cdot L_1 \cdot (\frac{1}{V_{in}} + \frac{1}{V_{Cc} - V_{in}}) .$$ (11)

Then, the hysteresis band width is:

$$h = \frac{1}{2}\Delta I_{L1} = \frac{V_{in}}{2L_1} \cdot D \cdot T_S ,$$ (12)

Due to the symmetry of the circuit, equation (13) will be obtained in accordance with the power conservation law.

$$I_{L1}^* = \frac{1}{2}I_{in}^* = \frac{1}{2} \cdot \frac{V_E \cdot I_o}{V_{in}} = \frac{1}{2} \cdot \frac{V_E^2 \cdot i_o(t)}{V_{in} \cdot v_o(t)} ,$$ (13)

where, I_{L1}^* is the theoretical average current of the input inductor L_1, I_{in}^* is the theoretical input current, V_E is the theoretical output voltage while $v_o(t)$ is the actual one, I_o is the theoretical output current while $i_o(t)$ is the actual one.
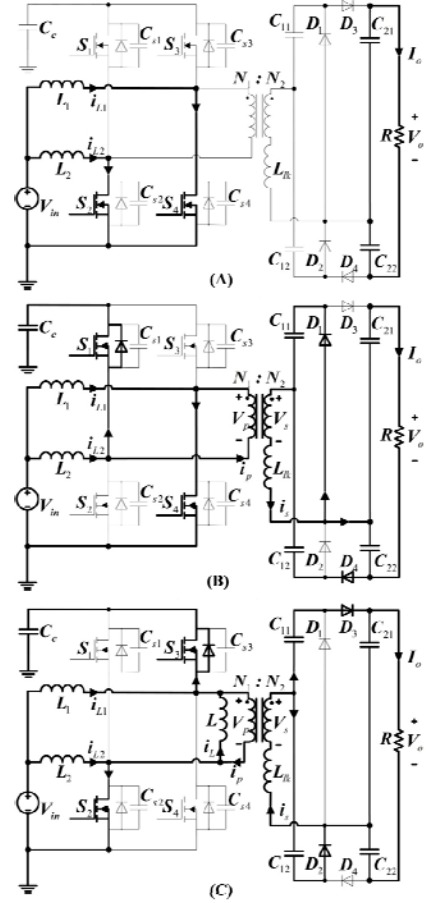

FIGURE II. OPERATION STAGES OF THE DC-DC CONVERTER. (A) STAGE1: S_2 ON, S_4 ON. (B) STAGE2: S_2 OFF, S_4 ON. (C)
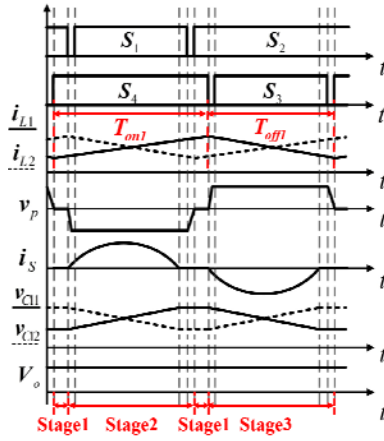
FIGURE III. KEY WAVEFORMS OF THE DC-DC CONVERTER DURING DIFFERENT STAGES

Operation stages of the DC-DC converter. (a)Stage1: S_2 on, S_4 on. (b) Stage2: S_2 off, S_4 on. (c) Stage3: S_2 on, S_4 off.

Key waveforms of the DC-DC converter during different stages

There is error between the theoretical output voltage and the actual one in applications. The error voltage ΔV_o is:

$$\Delta V_o = V_E - v_o(t) . \tag{14}$$

The error voltage ΔV_o works as a feedback quantity in the proposed PWM current hysteresis control scheme, and the error between the theoretical average current of the input inductor L_1 and the reference one can be calculated as (15).

$$\Delta i_{L1}{}^*(t) = \frac{[V_E - v_o(t)] \cdot I_o}{2V_{in}} = \frac{[V_E - v_o(t)] \cdot V_E \cdot i_o(t)}{2V_{in} \cdot v_o(t)} . \tag{15}$$

By combining (13) and (15), the reference current of the input inductor L_1 should be:

$$I_{L1} = I_{L1}{}^* + \Delta i_{L1}{}^*(t) = \frac{1}{2} \cdot \frac{[2V_E - v_o(t)] \cdot V_E \cdot i_o(t)}{V_{in} \cdot v_o(t)} . \tag{16}$$

Due to the symmetry of the circuit, the relationship between the reference current of the input inductor L_1 and L_2 is：

$$I_{L2} = I_{L1} = I_{ref} . \tag{17}$$

The proposed current hysteresis control system is presented in Figure 1. The input voltage V_{in}, the output current $i_o(t)$ and the output voltage $v_o(t)$ can be obtained by the sampling circuits. The reference current of the input inductor L_1 will be calculated by DSP according to (16). The hysteresis band width will be adjusted according to (12). When the actual

current of the input inductor L_1 is larger than the upper threshold, the output signal is in low level and the switch S_4 will turn off. When the actual current of the input inductor L_1 is smaller than the lower threshold, the output signal is in high level and the switch S_4 will turn on. When the actual current of the input inductor L_1 is between the upper threshold and the lower one, the switch S_4 will keep its state. The switching operations of S_4 are shown as (18) and S_3 is driven complementarily by S_4.

Similarly, the switching operations of S_2 are shown as (19) and S_1 is driven complementarily by S_2.

$$\left(\begin{array}{c} S_4 \ turn \ on, \ i_{L1} < I_{L1} - h \\ S_4 \ hold \ on, \ I_{L1} - h < i_{L1} < I_{L1} + h \\ S_4 \ turn \ off, \ i_{L1} > I_{L1} + h \end{array} \right) \tag{18}$$

$$\left(\begin{array}{c} S_2 \ turn \ on, \ i_{L2} < I_{L2} - h \\ S_2 \ hold \ on, \ I_{L2} - h < i_{L2} < I_{L2} + h \\ S_2 \ turn \ off, \ i_{L2} > I_{L2} + h \end{array} \right) \tag{19}$$

III. SIMULATION AND ITS RESULTS

A. Simulation Circuit

To verify the proposed PWM current hysteresis control scheme, the duty cycle of the switches S_2 and S_4 is set to 0.6 in this paper, and the simulation is carried on, as shown in Figure 4, The simulation model is composed of the DC-DC converter circuit (module 3 in Figure 4), the reference current calculated circuit (module 2 in Figure 4) and the PWM driving signal generated circuit (module 1 in Figure 4). According to (16), the reference current I_{ref} will be calculated with module 2 by collecting the output voltage V_o, the output current i_o and the input voltage v_{in}. Module 1 performs as a PWM driving signals generator. The currents of two input inductors i_{L1} and i_{L2} are compared with the reference current I_{ref} and two current differences will be obtained, respectively. The hysteresis band width h will be calculated according to (12), and then the RELAYs will generate 4 PWM driving signals of two switch bridges by comparing two current differences with the hysteresis band width, respectively. Taking the second bridge as an example, the switching operations are shown in Table 2, which are coincident with the analysis in section Ⅱ.

TABLE I.   THE CIRCUIT PARAMETERS

Parameter	Value
Power (P)	400W
Input voltage (V_{in})	20V
Switching frequency (f_S)	50kHz
Input inductor (L_1=L_2)	68μH
Parasitic capacitance ($C_{s1} - C_{s4}$)	2.2nF
Clamping capacitor (C_C)	22μF
Leakage inductance (L_{lk})	0.9μH
Transformer ratio (N)	1 : 1
Resonant capacitance (C_{11}=C_{12})	2μF
Output capacitance (C_{21}=C_{22})	220μF

TABLE II.   OPERATION STAGES OF RELAY

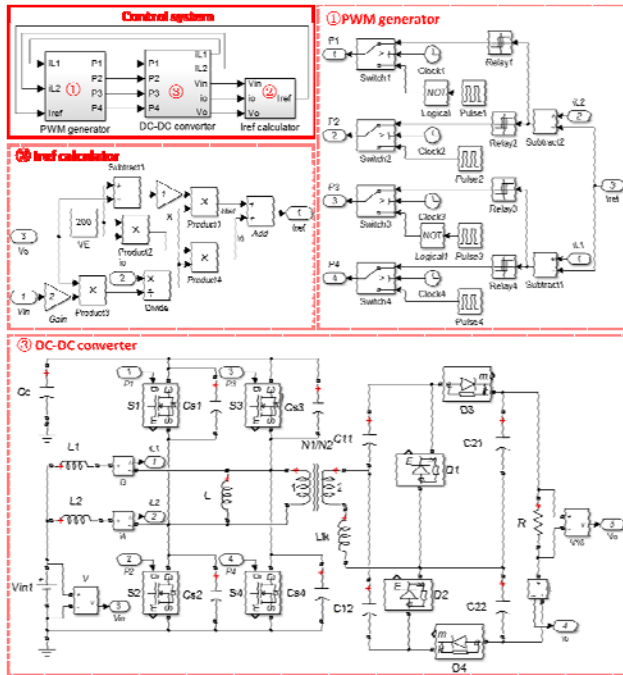|	Re$lay3(S_3)$	Re$lay4(S_4)$
$i_{L1} - I_{ref} > h$	1	0
$-h < i_{L1} - I_{ref} < h$	hold on	hold on
$i_{L1} - I_{ref} < -h$	0	1

FIGURE IV. SIMULATION MODEL OF THE DC-DC CONVERTER WITH CURRENT HYSTERESIS CONTROL SYSTEM

B.   Simulation Results

The theoretical output voltage is calculated to be 200V according to (12) and the parameters in Table 1. The theoretical current of the input inductor is 10A, which is half of the theoretical input current. The simulation waveforms of the output voltage and the input current are shown in Figure 5. The output voltage is around 194.7V, which is within an error of 3%, and the input current is 10.4A, which is within an error of 5%. Therefore, it has a high steady accuracy of 97%. In addition, the output voltage reaches a steady state at 0.02s, which means that the proposed current hysteresis control system has a speedy response.
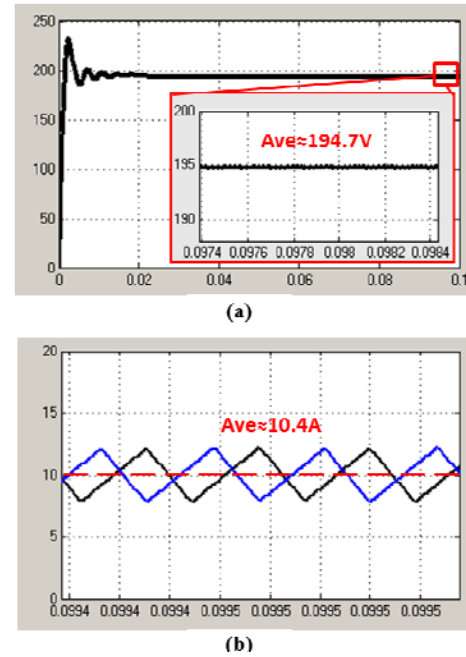

FIGURE V. SIMULATION WAVEFORMS OF THE DC-DC CONVERTER WITH CURRENT HYSTERESIS CONTROL SYSTEM. (A) SIMULATION WAVEFORM OF OUTPUT VOLTAGE. (B) SIMULATION WAVEFORMS OF INPUT CURRENT

Figure 6 presents the PWM driving signal of s_1 provided by module 1. The switching period is measured to be 20.633μs at 0.0258s and 20.702μs at 0.4867s. The error of two measured periods is about 3.5% compared with the theoretical period. The period fluctuation at two different times is really small as 0.07μs, which means constant-frequency control is obtained with the proposed current hysteresis control system.
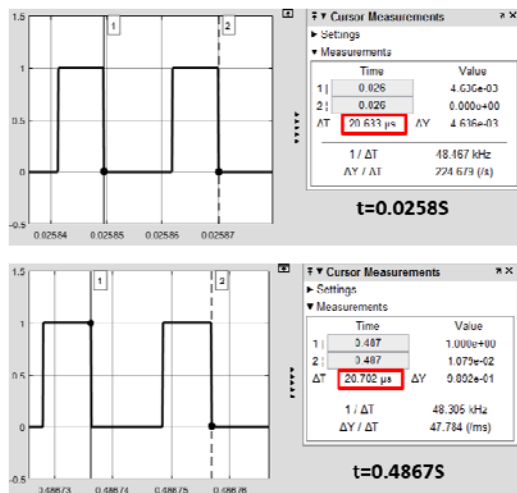
FIGURE VI. PWM DRIVING SIGNALS OF S_1 AT DIFFERENT TIMES

IV. CONCLUSION

This paper has proposed a PWM current hysteresis control scheme to improve the performance of the high step-up current-fed DC-DC converter in our previous work. The currents of two input inductors were treated as control quantities, and the error between the practical and theoretical output voltage was feedback quantity. The theoretical current of input inductor was calculated by collecting the output voltage and current of the DC-DC converter, and the hysteresis band width was adjusted in real time. Consequently, high quality steady output voltage waveform was obtained. The simulation results presented that the proposed PWM current hysteresis control is fairly easy to implement, and it has a speedy response and a high steady accuracy of 97%.

REFERENCES

[1] F. Haßler, F. Ellinger, U. Jörges, R. Wolf, and B. Lindner, "A high-speed buck converter for efficiency enhancement of W-CDMA power amplifiers." Int. J. Microw. Wirel. T. vol. 4, pp. 505-514, October 2012.

[2] R. Hou and A. Emadi, "A Primary Full-Integrated Active Filter Auxiliary Power Module in Electrified Vehicles with Single-Phase Onboard Chargers. " IEEE T. Power Electr. vol. 32, pp. 8393-8405, November 2017.

[3] C. Y. Chan, S. H.Chincholkar, and W. Jiang, "Adaptive Current-Mode Control of a High Step-Up DC–DC Converter." IEEE T. Power Electr. vol. 32, pp. 7297-7305, September 2017.

[4] Y. J. Park, J. H. Park, H. J. Kim, et al. "A Design of a 92.4% Efficiency Triple Mode Control DC–DC Buck Converter With Low Power Retention Mode and Adaptive Zero Current Detector for IoT/Wearable Applications." IEEE T. Power Electr. vol. 32, pp. 6946-6960, September 2017.

[5] S. S. I. Shakib and S. Mekhilef, "A Frequency Adaptive Phase Shift Modulation Control Based LLC Series Resonant Converter for Wide Input Voltage Applications." IEEE T. Power Electr. vol. 32, pp. 8360-8370, November 2017.

[6] B. Meghni, D. Dib, and A. T. Azar, "A second-order sliding mode and fuzzy logic control to optimal energy management in wind turbine with battery storage." Neural Comput. Appl. vol. 28, pp. 1417-1434, June 2017.

[7] M. Derbeli, M. Farhat, O. Barambones, and L. Sbita, "Control of PEM fuel cell power system using sliding mode and super-twisting algorithms." Int. J. Hydrogen Energ. vol. 30, pp. 8833-8844, March 2017.

[8] M.BV, "Fuzzy Controlled ZVS Asymmetrical PWM Full-bridge DC-DC Converter for Constant load High Power Applications." J. Electr. Eng. Technol. vol. 12, pp. 1235-1244, May 2017.

[9] A. Nouri, I. Salhi, E. Elwarraki, S. El Beid, and N. Essounbouli, "DSP-based implementation of a self-tuning fuzzy controller for three-level boost converter." Electr. Pow. Syst. Res. vol. 146, pp. 286-297, May 2017.

[10] L. Z. He, T. Zeng, et al. "High Step-up Active-Clamp Converter with an Input Current Doubler and a Symmetrical Switched-Capacitor Circuit." J. Pow. Electr. vol. 15, pp. 587-601, May 2015.

[11] R. Gavagsaz-Ghoachani, M. Phattanasak, M. Zandi, et al. "Estimation of the bifurcation point of a modulated-hysteresis current-controlled DC–DC boost converter: stability analysis and experimental verification." IET Power Electr. vol. 8, pp. 2195-2203, Nowember 2015.

[12] P. J. Liu, Y. M. Lai, P. C. Lee, and H. S. Chen, "Fast-transient DC–DC converter with hysteresis prediction voltage control." IET Power Electr. vol. 10, pp. 271-278, March 2017.

[13] S. Kapat, "Parameter-Insensitive Mixed-Signal Hysteresis-Band Current Control for Point-of-Load Converters With Fixed Frequency and Robust Stability." IEEE T. Power Electr. vol. 32, pp. 5760-5770, July 2017.